

Shape memory polyurethane - Amorphous molecular mechanism during fixation and recovery

A. Nissenbaum^{*}, I. Greenfeld, H.D. Wagner^{**}

Weizmann Institute of Science, Department of Materials and Interfaces, Rehovot, 7610001, Israel

ARTICLE INFO

Keywords:

Shape-memory
Strain-crystallization
Electrospinning

ABSTRACT

In this work, we investigate the governing fixation mechanism in a polycaprolactone-diol/2,4,2,6-Toluene diisocyanate/Ethylene glycol based shape memory polyurethane (SMPU). In particular, we test whether strain-driven crystallization, known to govern the SMPU fixation state in semi-crystalline SMPUs, is indeed vital for a significant memory capability. As synthesized, the SMPU exhibits semi-crystalline morphology. However, after heating, the synthesized semi-crystalline SMPU becomes amorphous and retains this state for up to 60 h, so that its crystallization is delayed. Consequently, this enables a complete shape-memory cycle without the effect of crystallization over the shape-memory properties. We show that in the amorphous state, the bulk SMPU displays substantial memory-effect capabilities approaching optimal performance, without contribution from crystallization mechanisms. This effect is further enhanced in electrospun SMPU nanofibers, likely as a result of the high molecular orientation induced by extensional flow. We propose that the dominant fixation and recovery mechanism in such SMPUs is the inhibition of molecular chain mobility, imposed by interlocking of the SMPU hard-segments when the polymer network is cooled below the transition temperature.

1. Introduction

Over the past decades, shape memory polymers (SMPs) have gained great attention due to many desirable characteristics such as programmability, low density, biodegradability and biocompatibility, low cost, large material selection, and easy processing [1,2]. Specifically, shape memory polyurethanes (SMPUs) have been extensively studied due to their diverse molecular designs and promising applications [3]. In general, SMPUs are phase-segregated polymers that combine two phases: a hard phase composed of a chain-extended urethane groups, and a soft phase composed of relatively low molecular weight amorphous or semi-crystalline polyol. The shape memory effect in these polymers is triggered by a series of thermomechanical actions around a transition temperature ($T_{\text{transition}}$), as illustrated in Fig. 1.

In terms of shape memory effect, the hard segments function as netpoints that memorize the permanent shape, due to either physical or chemical intermolecular bonds, whereas the soft segments act as a switch that enables the mobility of the molecular chains to a temporary deformed shape.

The effect of the degree of crystallinity over the memory capabilities

is discussed in literature. High degree of crystallinity is considered a prerequisite for a SMPU with high memory capabilities [3]. For example, Bothe showed that high shape fixation (i.e. the ability to fixate a deformed state) was exhibited with increasing degree of crystallinity in semi-crystalline polymers [4]. By the same token, Gunes et al. reported that the shape memory properties of shape-memory composites are reduced due to decreased crystallinity [5]. In addition to the degree of crystallinity, the phenomenon of strain-induced crystallization is also found to affect the shape fixation of SMPUs [6]. Strain-induced crystallization [7] arises when the polymer is deformed to relatively large strains during the programming phase. During this stage, the molecular chains are elongated and co-align closely, allowing crystallization to occur. Thus, when an SMP is deformed and subsequently cooled below the transition temperature (usually T_m in semi-crystalline SMPUs), the deformed state is fixed by the strain-induced immobile crystalline phase. Re-heating the SMPU above T_m melts the crystallites and allows the SMPU to recover its initial shape.

However, recent experiments have raised considerable ambiguity regarding the actual role of strain-induced crystallization in polymers, and whether the current theoretical knowledge is sufficient to explain

^{*} Corresponding author.

^{**} Corresponding author.

E-mail address: asaf.nissenbaum@weizmann.ac.il (A. Nissenbaum).

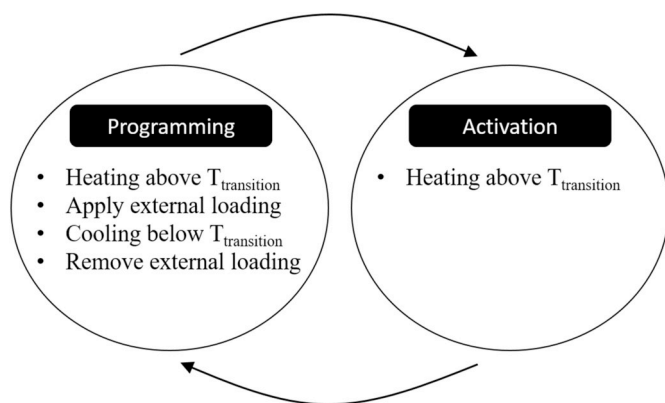


Fig. 1. Shape-memory transition schematic: the programming stage is aimed to bring the SMPU to a stable deformed state; the activation involves the exposure to a stimulus (in this case, heat) to recover the initial shape.

this phenomenon [8,9]. In the particular field of SMPs, Zue et al. have tried to analyze strain-induced crystallization in their polycaprolactone (PCL) based SMPU. They state that strain-induced crystallization was not observable and is likely to have only minor effect over the overall memory capability [10]. In addition, Pieczynska et al. have reported a consistent lack of strain crystallization in their tested SMPUs, regardless of changes in the experimental parameters [11]. Contrarily, Yan et al. reported that in a PCL-PIBMD SMP, strain-induced PCL domains were found to govern the shape memory process while the switching temperature was below T_m [12]. This duality rises from the versatility of SMP chemistry in general and SMPU in particular and suggests that these mechanisms are prone to variations due to the chemical constituents, morphology and processing conditions, and therefore, assumptions regarding the governing mechanisms in SMPs might in practice be inaccurate. Understanding the relation between the chemical procedure, morphology and subsequent memory capabilities is essential in terms of consistent assimilation to industrial needs.

The present work aims to clarify the role of the presence (or absence) of strain-induced crystallization in amorphous SMPUs. SMPU was synthesized catalyst-free, via a prepolymer method combining polycaprolactone-diol (PCL-diol)/2,4,2,6-Toluene diisocyanate (TDI) and ethylene glycol as a chain extender. The resulting semi-crystalline SMPU displays delayed-crystallization such that once heated, the SMPU becomes amorphous and retains this state for a long period. This ‘time-window’ in which the SMPU is completely amorphous enables to experimentally test whether strain-induced crystallization develops during the thermomechanical cycle and whether it serves as an acting mechanism in the SMPU. We also compared the bulk SMPU to electrospun SMPU fibers to understand whether the lack of strain-induced crystallization is a function of the amorphous phase topology, i.e. whether an amorphous electrospun SMPU will tend to crystallize under strain due to the pre-stretched molecular chains morphology.

The molar ratio between the diol groups and the diisocyanate groups is central for capable shape memory effect. An optimal stoichiometry ratio between the reactants has been proposed in the literature to be between 1:3–1:6 diol/Diisocyanate, depending on the chemical constituents of the polyurethane. This ratio assures a low degree of physical crosslinking that retains the required elasticity and strength [13] with less of an impact over the shape-memory performance. Increasing the physical crosslinking increases the polyurethane rigidity, resulting in inferior elasticity and shape memory properties. In the present study, the diol/diisocyanate ratio was 1:6, a stoichiometry ratio of reactants that has been proven to lead to considerable shape memory capabilities [14].

The formation of SMPU and the analysis of the hard segment-soft segment bonding was carried out by Nuclear Magnetic Resonance (NMR) and Attenuated-total-reflection Fourier-transform-IR (ATR-FTIR). The viscoelastic characterization and determination of T_g were

carried out by Dynamic mechanical analysis (DMA). The degree of crystallinity was analyzed by differential scanning calorimetry (DSC) and X-ray diffraction (XRD). XRD was also used for the analysis of time-dependent crystallization. Strain-induced crystallization was analyzed by DMA coupled with DSC to allow temperature controlled pre-stretching prior to the morphological analysis. DMA was also used to analyze the shape memory effect in the synthesized SMPU. The results show that the shape-memory process of the synthesized SMPU occurs during a time-scale in which the SMPU is completely amorphous. Thus, the process does not involve strain-induced crystallization, while still displaying high shape fixity and shape recovery values. This effect was also demonstrated in electrospun SMPU fibers that displayed a minimal strain-induced crystallized phase (0.44%). Our results demonstrate that in the absence of crystallization, the acting ‘amorphous’ mechanism involves the interlocking of hard segments that fixates the SMPU. In our study, the implementation of asymmetrical TDI coupled with a short EG chain extender, is leading to both steric hindrances and low mobility that not only induce stereo-irregularity that is realized in amorphous morphology, but also contribute to a better molecular interlocking, even at temperatures higher than T_g . We propose that the type and effect of the fixation mechanism can be tuned by the interplay between the composition of the hard and soft segments.

2. Experimental

2.1. SMPU synthesis

The SMPU was synthesized via the prepolymer method. An illustration of the synthesis scheme is displayed in Fig. 2:

ϵ -polycaprolactone (ϵ -PCL) diol (Leapchem, China) with a molecular weight of 2000g/mol was dried in a vacuum oven at 45 °C/24 h prior to the reaction. 80%/20% 2,4/2,6- toluene diisocyanate (TDI) and dehydrated ethylene glycol (EG) (Alpha Aesar, England), were dried with 4 Å molecular sieves. Dry toluene (Sigma-Aldrich) was used as a solvent. The synthesis of SMPU was carried out in a three-neck cylinder, equipped with Teflon magnetic stirrer, thermometer and Argon gas inlet and outlet. All addition of reagents during the synthesis reaction were carried out under an Argon flow. First, the reactor was washed with Ar gas for 20 min. ϵ -PCL-diol was dissolved in dry toluene at a ratio of 1:2 parts respectively. After the dissolution of PCL, a stoichiometric portion of TDI (6:1 TDI:PCL) was added dropwise at a rate of approximately 0.3 mL/min under rigorous stirring. The solution was kept on rigorous stirring for 90 min at 65 °C. A stoichiometric portion of EG (5:1 EG:PCL) was added at a rate of approximately 0.3 mL/min at the same conditions for another 90 min. After 70 min, the temperature was increased to 120 °C. The reaction solution was then removed from the reactor, poured into aluminum plates, and was degassed for 10 min. Then, the polymer was placed in an oven at 120 °C/14 h followed by additional 10 h at 35 °C.

2.2. SMPU characterization

2.2.1. Nuclear magnetic resonance (NMR)

The molecular structure of the synthesized SMPU was determined by ^1H NMR (Bruker AVANCE III, 300 MHz). Spectral width of 20 ppm was acquired with 16k points (Td) resulting in a resolution of 0.7 Hz.

2.2.2. ATR-FTIR

The chemical structure and presence of hydrogen bonding in the SMPU samples were evaluated by Bruker ALPHA FTIR equipped with diamond crystal ALPHA-P ATR module. The spectral data were collected from 400 to 4000 cm^{-1} with a 4 cm^{-1} resolution over 24 scans.

2.2.3. Differential scanning calorimetry (DSC)

The thermal transitions of the SMPU were analyzed using DSC (Q200, TA Instruments). The samples were heated from -40 °C to 200 °C at a 10 °C/min rate in a heat-cool-heat cycle.

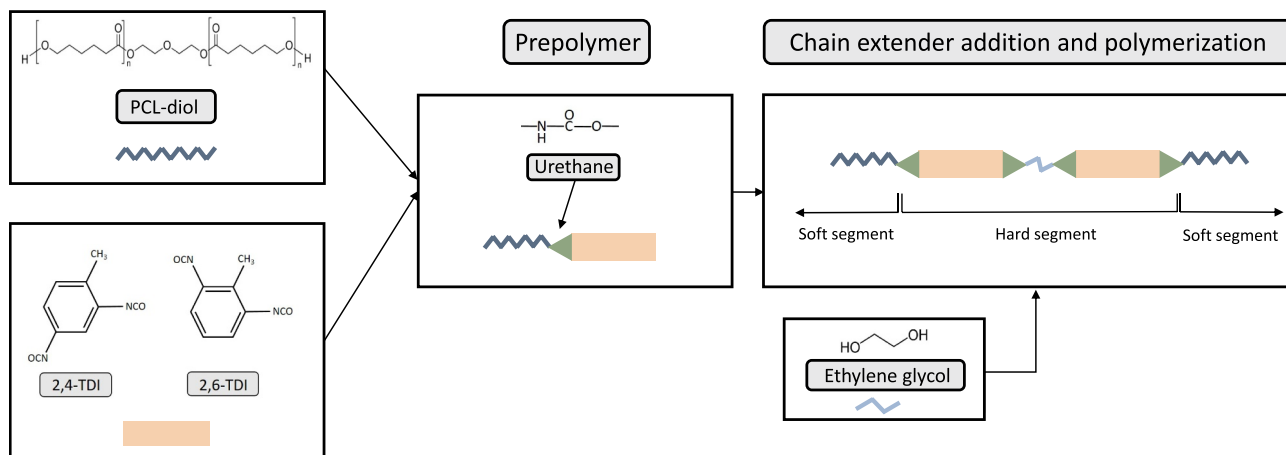


Fig. 2. Prepolymer synthesis of SMPU.

2.2.4. Dynamic mechanical analysis (DMA)

The viscoelastic behavior of the SMPU were studied using DMA (Discovery850, TA Instruments). The samples were measured in an oscillatory tensile mode at a frequency of 1 Hz at a heating rate of 3 °C/minute over the range of -70 °C–180 °C. The storage modulus and loss modulus values were recorded against temperature.

2.2.5. X-ray diffraction

XRD measurements of SMPU crystallinity and in-situ crystallization were measured with Rigaku TTRAX III (18 kW) theta-theta vertical diffractometer equipped with Cross Beam Optics (Tokyo, Japan), at 50kV/200 mA. The data collection was performed in the range $2\theta = 1-60^\circ$ with a step of 0.0250. The time-dependent XRD measurements were taken at intervals of approximately 90 min, and ended when sequential crystallization was observed for a few consecutive times.

2.3. Preparation of electrospun SMPU nanofibers

Electrospinning of the synthesized SMPU nanofibers was carried out using a custom-made apparatus as follows. First, the SMPU film was dissolve in DMF for 24 h to a 25%wt solution. The solution was then moved to a 1 mL glass syringe with an 18G needle. The flow rate was controlled by a syringe pump (LongerPump, Precision pump inc.) and was set to 1 mL/h. The distance between the syringe and the collector was set to 15 cm and the applied voltage was set to 16 kV. The temperature and humidity inside the electrospinning-designated hood were 25 °C and 60%RH respectively. The target collector in this experiment was a rotating drum controlled by an external power source (Cintex). An image of the custom-made system is display in the supplementary section (Fig. S1).

2.4. Shape memory characterization

A force-controlled thermomechanical cycle for evaluating the shape-memory response of bulk SMPU and electrospun SMPU nanofiber mat were conducted using DMA (DMA Q800, TA instruments) in tension mode. The shape-memory cycle is conducted such that non-recoverable deformations will not occur. The procedure is as follows:

- 1) The SMPU was equilibrated at 70 °C for 10 min.
- 2) A force-rate ramp of 0.1 N/min to 1N was applied.
- 3) The SMPU was cooled to 0 °C at a 5 °C/min cooling rate and was held isothermally for 45 min.
- 4) The applied force was released at a 0.50 N/min to 0.0010N rate and was held isothermally for 15 min.

- 5) The SMPU was reheated to 70 °C at a 5 °C/min rate and was held isothermally for additional 45 min.

Bulk sample were in average 4mm × 1mm × 10mm [width, thickness length]. Film samples were 0.05–0.1mm × 7mm × 7mm. Four samples were made for each experiment.

2.4.1. Calculation of shape memory fixity and recovery

SMPs are characterized by two main parameters: shape fixity and shape recovery. Shape fixity describes the ability to store strain (i.e. to fixate a deformed state) at temperatures below the transition temperature. Thus, it can be defined as:

$$R_f\% = \frac{\epsilon_u}{\epsilon_m} * 100\%$$

Where ϵ_m is the maximum strain and ϵ_u is the strain fixed after cooling and unloading. Shape recovery describes the ability to recover strain at temperature range that exceeds the transition temperature. It is defined as:

$$R_r\% = \frac{\epsilon_r}{\epsilon_m} * 100\%$$

Where ϵ_r is the residual strain after activation, given by $\epsilon_r = \epsilon_u - \epsilon_p$ where ϵ_p is the recovery strain.

Strain-induced crystallization analysis was carried out by coupling DMA and DSC:

- (1) The temperature in the DMA chamber was equilibrated at 65 °C.
- (2) The sample was stretched to 150% at a strain rate of 10%/min.
- (3) The sample was cooled to -100 °C at a rate of 150 °C/min
- (4) The sample was transferred to DSC and a heat scan was initiated from -40 °C to 100 °C.

3. Results and discussion

3.1. Chemical composition and structure

The chemical structure of the polymerized SMPU was confirmed by ¹H NMR (Fig. 3a) and supported by further ATR-FTIR analysis (Fig. 3b). In addition ATR-FTIR was used to assess the potential physical cross-linking within the SMPU chains.

The chemical structure in Fig. 3a represents a typical repeating unit of 2,4-TDI isomer that is likely to be the predominant isomer within the bulk material. The peaks at 8.9–9.7 ppm (f) correspond to different types of urethane groups (that originate from the possible modes of the 2,4 and 2,6 TDI isomers) [15,16]. CH₃ proton of the TDI units are shown as a

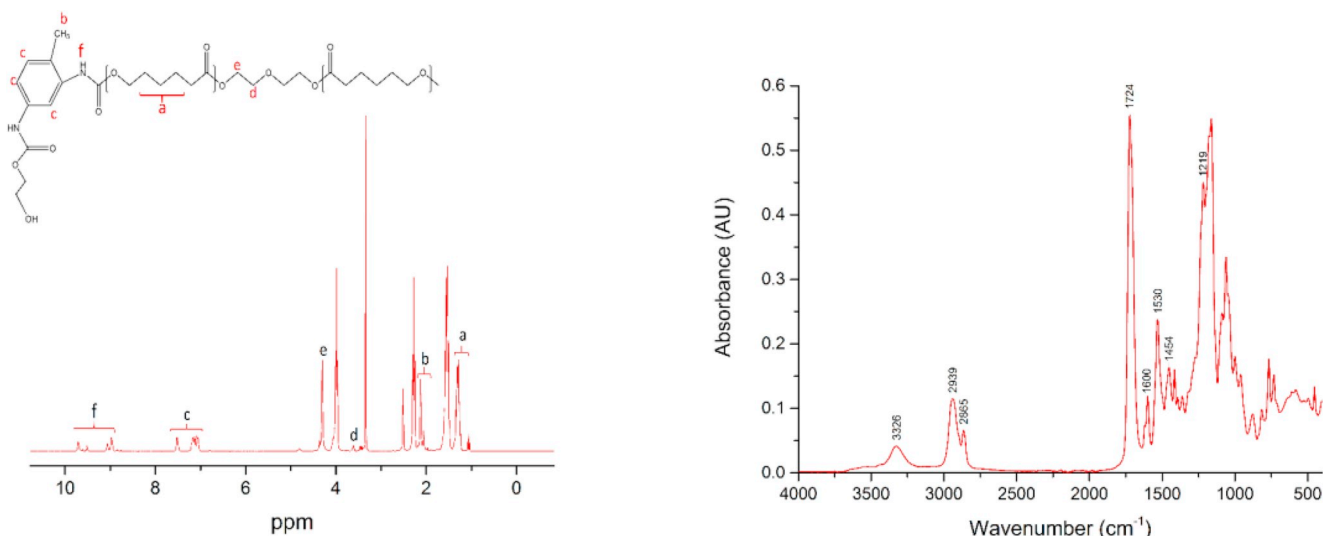


Fig. 3. (a) ¹H NMR spectrum. The inset in figure displays a typical repeating unit of the SMPU. (b) FTIR spectrum of the SMPU.

doublet at 2.0 and 2.1 ppm (b). The peaks at 7–7.5 ppm correspond to the aromatic hydrogens of 2,6 and 2,4 TDI respectively (c). The peaks at 1.3–1.6 ppm (a) correspond to the -CH₂ groups in the PCL chain together with the CH₂ group adjacent to the PCL carbonyl visible at 3.9 ppm [17]. The protons of the short aliphatic chain that connects two PCL chains is displayed at 3.6 and 4.2 ppm [18] (d,e). These aliphatic chain peaks are likely to overlap with the chemical shift of the ethylene glycol chain extender that is shown at ~4.0 ppm [18]. The peaks at 2.5 and 3.3 are assigned to the DMSO and DMSO water, respectively.

ATR-FTIR was used to investigate the SMPU synthesis. The lack of a stretching peak around 2200 cm⁻¹ indicates that the reaction was completed as no isocyanate reactant is detected. Furthermore, the peaks at 3326 cm⁻¹ and 1600 cm⁻¹ indicate the stretching vibration and in plane bending of N-H, respectively. The absorption peak at 1724 cm⁻¹ is associated with the C=O in the PCL as well as in the urethane group, and the 1219 cm⁻¹ peak is associated with the benzene C=C bond. The peaks at 2865 cm⁻¹ and 2939 cm⁻¹ indicate the soft-segment CH₂. The peaks at 1454 cm⁻¹ and 1530 cm⁻¹ are associated with the C-N and CH₂ bonds respectively, further supporting the signature of polyurethane. The extent of physical crosslinks in the SMPU is indicated by the amount of NH groups forming a crosslink, either between hard segments, or between soft and hard segments. It has been shown previously that peaks around 3420 cm⁻¹ and 3320 cm⁻¹ are attributed to free NH and bonded NH groups, respectively [19].

Our results display a strong peak at 3326 cm⁻¹ with no apparent peak around 3420 cm⁻¹. Followed by the work of Wang et al. [20], we used Origin software to deconvolute the broad peak of 3326 cm⁻¹ in attempt to see whether this peak overlaps several additional NH bonds. However, the result does not indicate overlapped NH peaks at 3326 cm⁻¹. This serves as a clear indication that the NH groups of the urethane segments are predominantly bonded, hence increasing the amount of netpoints in the SMPU.

The high density of netpoints is expected to improve the integrity of the network during the programming and recovery phases. Furthermore, it was shown previously that the peak around 1720 cm⁻¹ indicates the hard segments-soft segments bonding while the characteristic peak at 1690 cm⁻¹ indicates hard segments-hard segments bonding [21].

Our results show a single broad peak at 1724 cm⁻¹. This corresponds well with polyesters such as PCL, which is a strong hydrogen-bond acceptor and therefore is prone to interact with the urethane NH group. This translates to excess of netpoints between hard and soft segments, and relates to the decrease in the degree of crystallinity due to misalignment between the hard segments. The resulting chemical

composition of the SMPU makes it possible to investigate the shape memory function of a completely amorphous SMPU, without the interference of the different effect of crystallinity.

3.2. Thermal and morphological characterization

DSC was used to characterize the thermal properties of the SMPU. XRD was used to characterize the morphology of the SMPU as well as a supporting method for the DSC findings (Fig. 4):

The DSC graph describes a heat-cool-heat experiment. The first heating of the synthesized SMPU displays a crystalline phase (Fig. 4 left – the red dashed curve) with melting temperature $T_m = 48$ °C. This result coincides with the crystalline phase and the melting temperature (T_m) of ϵ -PCL. By contrast, additional cooling and reheating do not display any recrystallization and the second heating displays an amorphous thermogram. We further verified this behavior using XRD (Fig. 4 right). In the XRD, we compared ‘as synthesized’ SMPU diffractogram (Fig. 4 right, red curve) to heat-treated SMPU, heated to 65 °C and cooled at R.T overnight. We see that the peaks in the as-synthesized SMPU, which indicate crystallinity, are absent from the heat-treated SMPU. It is visible that within the cooling time-scale the SMPU has remained amorphous.

The ‘as-synthesized’ crystallinity (19%) is likely the result of the amount of solvent used during synthesis and the lack of catalyst. With regard to the former, the SMPU was synthesized using 2:1 parts toluene per solute. Toluene dissolves the less polar PCL-diol but is less effective for the more polar aromatic TDI. Therefore, during polymerization the hard segments have higher potential for crystallization. However, once the fully synthesized SMPU is reheated, the potential for crystallization in the absence of the solvent contribution is lower. It was substantiated in the literature that the isocyanate group has a strong impact over the molecular chain symmetry that subsequently affects the degree of crystallization. TDI in particular was found to enforce structural interruptions that tend to decrease the degree of crystallization [22–24]. With regard to the chain-extender EG, although there are relatively few SMPU synthesis that involve EG (with respect to longer chain extenders), it was reported that such a short diol causes contraction and prohibits the packing of hard segments to oriented crystals [25]. Therefore, the coupling of the asymmetrical TDI groups with the short EG dictates spatial chain disorder that reduces oriented packing of hard segments and shifts the degree of crystallinity further toward a low-order, amorphous morphology. Furthermore, the relatively low molecular weight PCL-diol can also inhibit crystallization to some extent

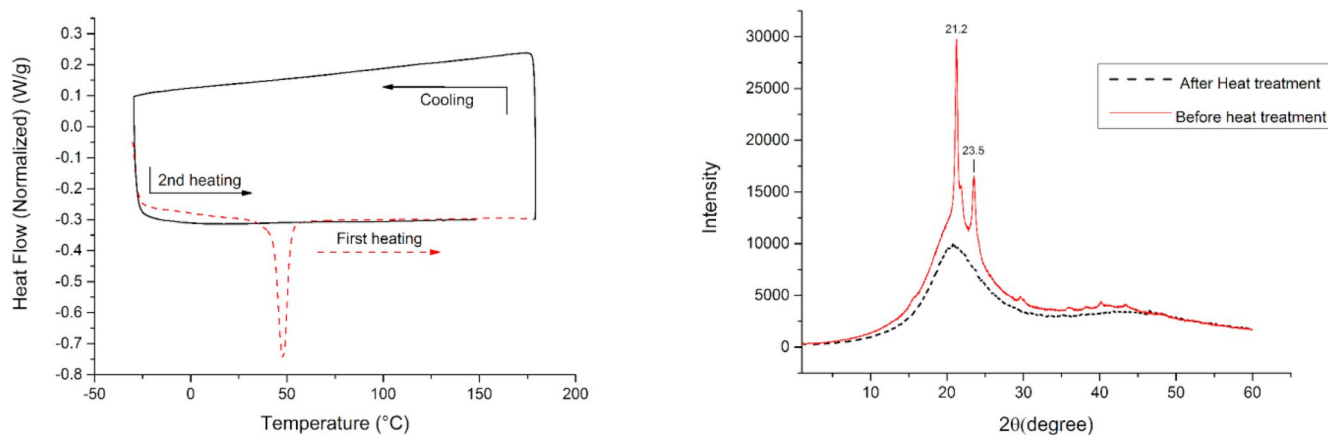


Fig. 4. Thermal and morphological properties of the SMPU. Left - DSC thermogram of bulk SMPU. Right - XRD diffractogram of bulk SMPU before and after heat treatment.

due to preference of hard-segment/soft-segment bonding [26] as seen in the FTIR results. When such preference occurs, the symmetry of the SMPU chains decreases as the hard segments and soft segments will not tend to crystallize.

3.2.1. Delayed crystallization

Over a period of time, an increase in the rigidity of the SMPU was observed, suggesting that crystallization reoccurred. Therefore, an in-situ XRD experiment was carried out to identify the time scale in which the amorphous SMPU initiates crystallization (Fig. 5). We note that although there are reports that claim that cold crystallization might occur in 2,4-TDI based polyurethanes over time [27], neither estimation of this time-scale nor the extent of crystallinity were reported. The time dependent crystallization is displayed in Fig. 5:

Fig. 5 reveals three states of morphology changes (indicated by numbers): During the first 2 h (region 1, green curve), the SMPU gained a minimal degree of order toward a long-term, low order morphology. Then, at room temperature, a steady state (region 2, blue curves) remained for approximately 60 h, followed by recrystallization (region 3, brown curves). Although such complex phenomenon depends on several factors, we note that this result was achieved with PCL-diol as a soft segment, known to produce higher degree of crystallinity [28]. This

unique phenomenon is likely the result of slow chain relaxation at the RT regime. The amorphous polymer has low-mobility hard segments that constrain the relaxation of the soft chain segments. However, given enough time in a temperature above T_g , chain relaxation was sufficient for the chain segments to move and co-align, resulting in recrystallization.

To summarize these findings, we show that in our synthesized SMPU, heat treatment removes the primary crystallization and the SMPU becomes amorphous. The amorphous conformation is likely caused by the low symmetry that is imposed by the TDI-EG hard segment and the intermolecular hard segment-soft segment bonding. However, over time (~ 60 h) slow chain relaxation is translated to recrystallization of the SMPU. In the particular interest of this work, the time-scale in which the shape-memory cycle takes place is well within the amorphous state of the SMPU, such that no crystallization is involved in the tested shape-memory process.

3.2.2. Strain-induced crystallization (SIC)

Since the SMPU is amorphous after heat treatment, it provides the ability to detect experimentally the manifestation of strain-induced crystallization as a possible fixation mechanism of the SMPU. It was reported that TDI based polyurethane displays strain-induced

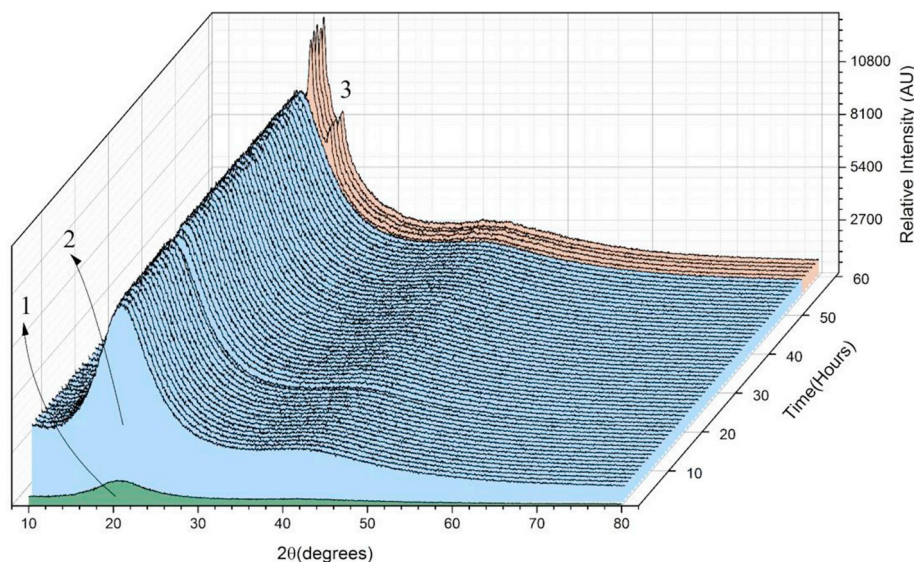


Fig. 5. XRD diffractogram over a period of 60 h after heat treatment. It is visible that the SMPU is amorphous for over 50 h (designates by regions 1 and 2) before recrystallization initiates (region 3).

crystallization at a relatively low strain of $\sim 110\%$ while for instance MDI-based polyurethane exhibits SIC at much higher strains [29]. However, as discussed earlier, the chemical constituents and synthesis processing affect the extent of crystallization. Since we assume that the stereo-irregularity of the hard segments inhibits molecular orientation and crystallization, we also analyzed electrospun fibers, which were processed from the same bulk SMPU as a comparable system with a high degree of molecular orientation. These analyses are displayed in Fig. 6.

Fig. 6a displays the ‘as-prepared’ crystallization state of the bulk and electrospun specimens. Electrospun fibers gain high molecular stretching due to the forced orientation imposed by the spinning process, which in turn increases their crystallinity. Fig. 6b displays the heat-treated specimens and show similarly to the bulk SMPU, a heat treatment completely removes the crystalline phase from the electrospun samples. Fig. 6c displays the strain-induced crystallization of the bulk and electrospun SMPU. Under moderate strains (150%), the bulk SMPU does not display strain-induced crystallization, whereas the electrospun SMPU displays a minimal crystalline phase of 0.44%. These results correspond with our hypothesis that this SMPU is highly disordered, preventing crystallization from taking place. The strain-induced crystallization caused by the pre-stretching of the electrospun fibers seems negligible with regards to the shape-memory function. These results validate that the SMPU remains amorphous throughout the shape-memory cycle, without the involvement of crystallization.

3.3. Viscoelastic properties

The mechanical impact of removing the crystalline phase on the viscoelastic properties of the SMPU was measured by DMA for both treated and un-treated SMPUs (Fig. 7). Under dynamic loading, the storage modulus reflects the degree of stored elastic energy (Fig. 7b), whereas the loss modulus reflects the dissipated viscous energy (Fig. 7c); the damping phase angle represents the ratio between the loss and storage moduli (Fig. 7a).

In the semi crystalline states below T_m , the viscous movement of the molecular chains is repressed by the existence of immobile crystallites and therefore only a mild decrease of the storage modulus occurs when the temperature is increased and elasticity is retained even above T_g (Fig. 7b). Above T_m , the crystallites melt and this mobility barrier is removed, consequently causing a rapid drop in the storage modulus. By comparison, this mechanism does not exist in the amorphous state where the molecular chains gain their mobility immediately after T_g and exhibit a sharp decrease in the storage modulus. In both the semi-crystalline and amorphous SMPUs, the elasticity of the cross-linked network is still retained at high temperature, regardless of the loss due to the viscous mobility of chains; this is seen in the region above $\sim 60^\circ\text{C}$ in both SMPU types.

T_g was calculated by observing the peak of the loss modulus (Fig. 7c). The shift in T_g between the amorphous and crystalline states is likely a result of the interfacial forces between the crystalline and amorphous phases; strong interfacial bonding between the amorphous

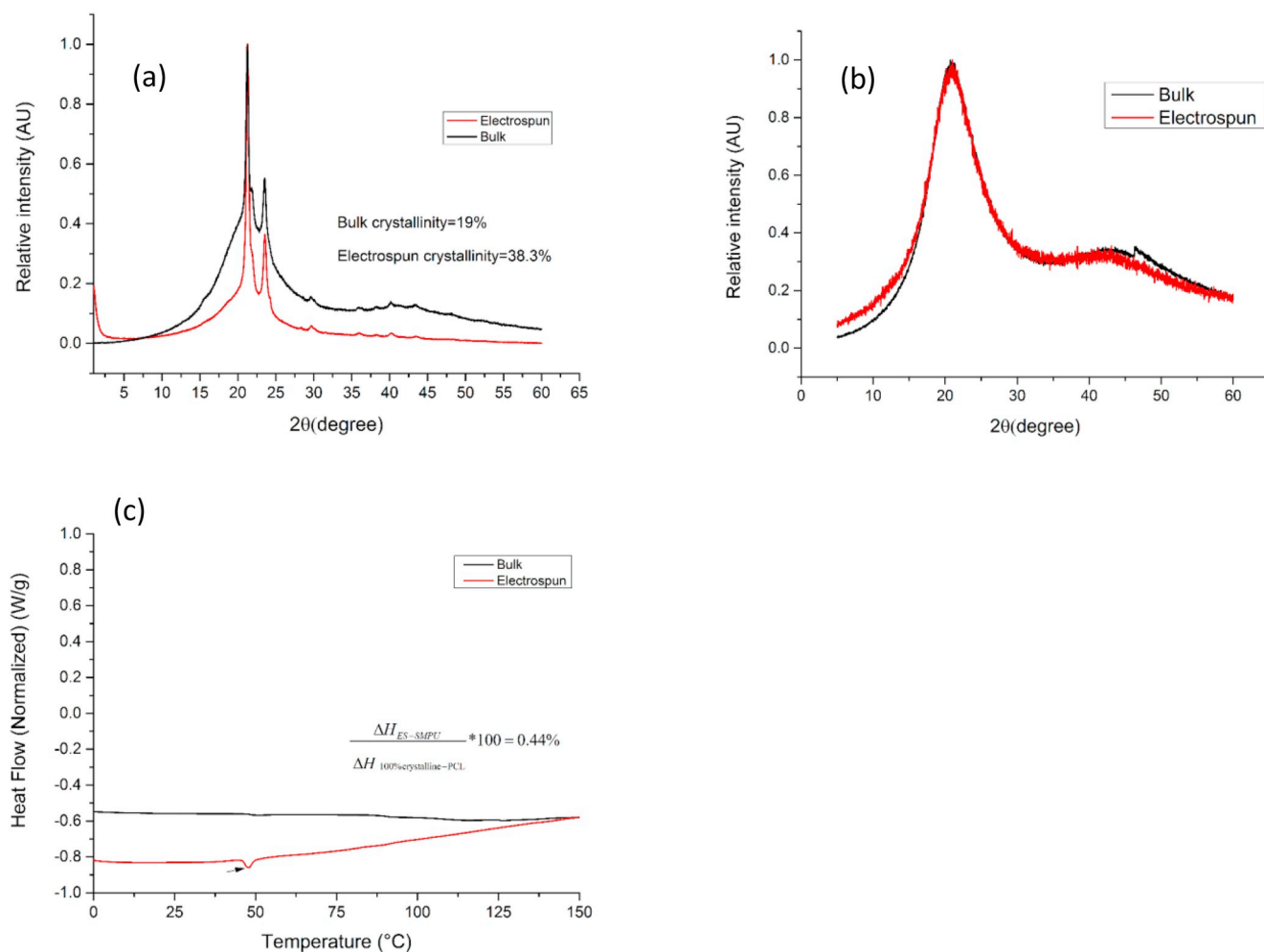


Fig. 6. Strain-induced crystallization in electrospun SMPU. (a) XRD diffractogram of ‘as-synthesized’ bulk and electrospun SMPUs and (b) their diffractogram after heating. (c) Strain induced crystallization observed in DSC.

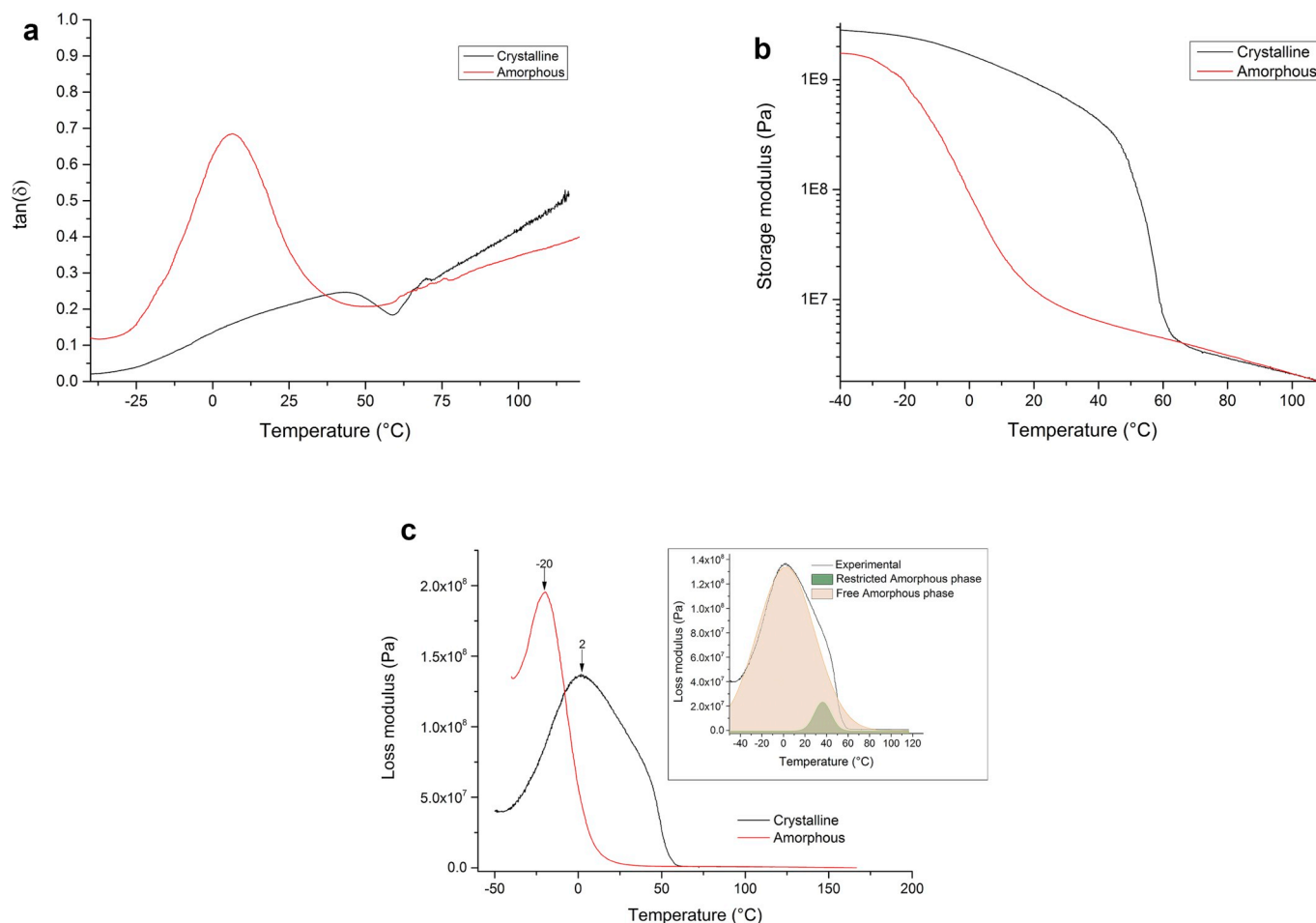


Fig. 7. Viscoelastic properties of the SMPU amorphous and crystalline states. (a) $\tan(\delta)$ measurements of the damping capacity (phase lag between stress and strain). (b) Storage modulus measurements. (c) Loss modulus through which T_g was calculated. The inset graph is a computer-aided deconvolution of the crystalline loss modulus peaks, which shows two modes of energy dissipation.

and crystalline phases induces constraints that increase the energy required to cause viscous movement of the amorphous chains in that interface. Computer-aided analysis of the semi crystalline loss modulus peak display two energy dissipation modes (Fig. 7c, inset): The brown peak is attributed to the amorphous phase far from the amorphous/crystalline interface, whereas the smaller green peak can be attributed to the amorphous chains in the vicinity of the amorphous/crystalline interface [30].

The $\tan(\delta)$ measures the damping capacity of the polymer (Fig. 7a), displaying a significant difference between the two states: the crystalline SMPU displays low damping with maximum peak height of 0.18 close to T_m , whereas the amorphous SMPU displays a wide peak with maximum height of 0.67 which is comparable to the damping of elastomers. The possibility of switching between high-damping and low damping states by external switch, in this case by varying the temperature, is a desirable property in state-devices such as vibration absorbers.

In summary, the analysis above reflects the conceptual difference of the shape-memory mechanism between semi-crystalline and amorphous SMPUs. The shape memory mechanism in the amorphous SMPU is predominantly viscoelastic, namely the state of the polymer chains during the programming and recovery is governed by their elasticity as well as by their viscous mobility in the frictional dissipative environment created by their neighbors. By contrast, the semi-crystalline shape memory mechanism involves storage and release of elastic energy through crystallization and crystallites melting, respectively.

3.4. Shape memory performance

Fig. 8 displays a shape-memory cycle of the bulk and electrospun SMPUs.

As stated, the time frame of the test is well within the amorphous mode of the SMPU, and consequently, crystallization phenomena do not affect the memory parameters. Therefore, the sole mechanism that acts on the SMPU is the interlocking of hard-segment mobility while cooling down toward T_g . The bulk SMPU displays good memory capabilities with shape fixity of 89% and shape recovery of 93%, comparable with SMPUs that involve a crystallization mechanism [31,32]. The electrospun SMPU displayed superior shape memory parameters with 99% recovery and 97% fixity. We may conclude that with respect to the shape fixity and recovery, an amorphous SMPU can perform as well as a crystallized SMPU. In other words, despite being amorphous, the polymer network provides efficient interlocking of hard segments in the fixated state, while keeping the network integrity, so that when the SMPU is recovered, hard segments are released and allow almost complete recoiling of the network to its initial state.

The relaxation time constants were estimated at the recovery isothermal state, assuming viscoelastic exponential decay, to be 8.3 and 14.2 min for the electrospun and bulk SMPU, respectively (Fig. 8b). The difference can be attributed to the lower entanglements density in the electrospun SMPU compared to the bulk SMPU. In the electrospun SMPU, the extensional flow during the electrospinning process promotes disentanglement, causing chain segments between entanglements to be longer, consequently decreasing the confinement of chains [33,34]. Less

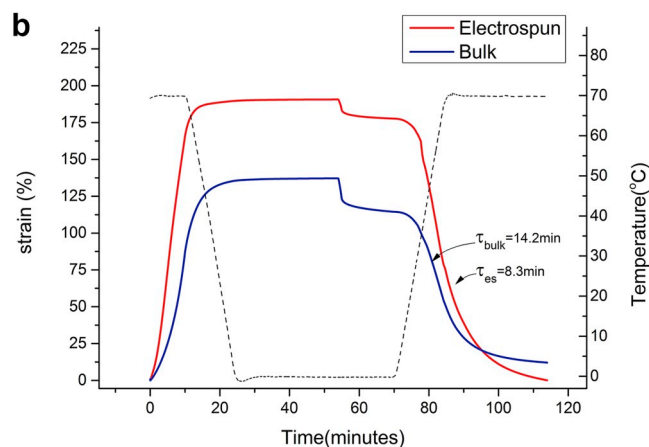
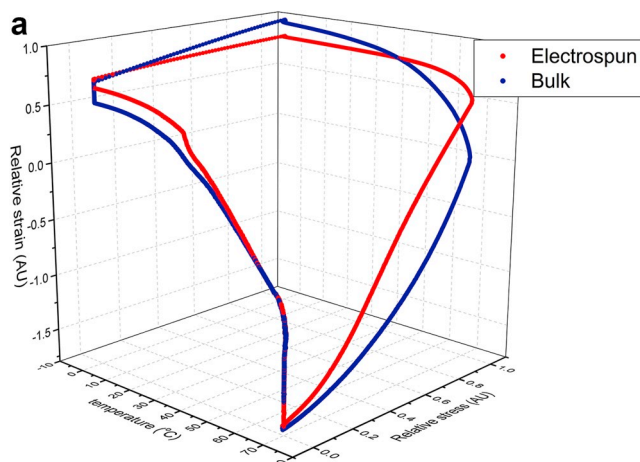


Fig. 8. Shape-memory cycle of the bulk and electrospun SMPUs. (a) 3D representation of the temperature and normalized stress and strain. (b) Strain profile (solid lines) and temperature (dashed line) as functions of time. The recovery characteristic times are indicated.

confinement is associated with shorter relaxation times, and therefore the less confined electrospun SMPU will have a shorter relaxation time. This also explains the appearance of some strain-induced crystallinity in the electrospun SMPU, where the less entangled polymer chains can co-align more easily and crystallize. The increase in shape fixity of the electrospun SMPU is usually attributed to the morphology of the electrospun SMPU [35]. Particularly, electrospun SMPU have higher degree of molecular orientation, and the free space between adjacent chains is smaller. Thus, after fixation, the molecular chains are more restrictive and reduce the degree of fixity degradation.

3.5. Shape memory mechanisms

The SMPU in its amorphous state is a polymer whose chains are primarily flexible but contain relatively long hard segments. These chains create a network through formation of crosslinks (netpoints) between adjacent chains. These crosslinks consist of hydrogen bonds between the hard-soft segments and hard-hard segmental groups. During programming, the network is heated to a temperature that allows mobility of chain sections between crosslinks, without harming the integrity of the network (that is, crosslinks are not broken). Once decreasing the temperature for fixation (while remaining above T_g), the hard segments which are relatively long and rigid, make it hard for the chains to move with respect to each other, resulting in a fixated state of the network. When the temperature is increased for the purpose of recovery, the hard segments are no longer entrapped and allow chains to move more freely. At this point, the network will recover to its initial coiled state. For convenience we will refer to this process as the ‘amorphous’ mechanism, to distinguish it from the shape-memory mechanism that is based on crystallinity. An illustration of this mechanism is displayed in Fig. 9.

The mobility of a chain-segment that is constrained between two crosslinks is dependent on the available space confined by the surrounding chains, and is depicted in the illustration (Fig. 9). (a) as a tubular volume element surrounding a typical constrained chain segment. The notion of a confinement tube is commonly used in polymer physics to express the restrictive potential imposed on a mobile chain by its neighbors, allowing the chain to move within it by viscous reptation [36]. At a highly entangled dense state, for example when the temperature is relatively low, the confinement tube is thinner (Fig. 9b), and therefore, the mobility of “bulkier” hard segments is hindered. At this state, the hard segments are immobile, in other words, interlocked within the “walls” of the confinement tube, and as a result the SMPU shape is fixated. At an elevated temperature, such as during recovery or programming, the space around the chain is less confined, allowing free

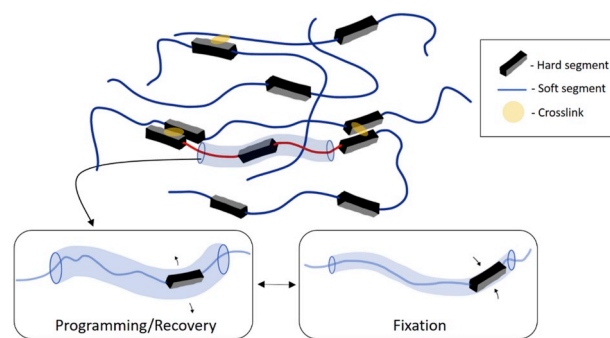


Fig. 9. Illustration of the amorphous fixation mechanism of an SMPU. (a) General schematic of the SMPU with a tubular confinement volume around a typical SMPU chain. (b) State of the confinement tube during the programming or recovery steps. (c) State of the confinement tube as a result of fixation.

movement of the entire chain segment including the hard segments (Fig. 9b). When the hard segments mobility decreases, phenomena such as strain recovery, relaxation, creep and so forth require higher temperature or equivalently longer time to take place. In our system, we coupled TDI, which is a low mobility hard segment with EG which is the shortest diol chain extender. The coupling of such elements further decreases the mobility of the hard segments, whereas longer chain extenders were found to increase the hard segment mobility [37].

In general, crystallinity can provide an additional fixation mechanism by preventing the mobility of chain sections that were crystallized. We suggest that both the amorphous and crystalline mechanisms are in general simultaneously in action in SMPUs, and their relative impact is governed by the chemical composition and stoichiometry of the SMPU. Thus, in systems that are comprised of symmetrical hard segments (such as symmetrical aromatic diisocyanate or aliphatic diisocyanate) and relatively long soft segments, we can expect crystallinity to be the dominant mechanism, whereas in systems with asymmetrical hard segments and relatively short soft segments the amorphous mechanism will predominate. For example, Kojio et al. [38] have reported that the addition of methyl groups on the soft segments can repress strain-induced crystallization. Additionally, by varying the length and composition of the soft and hard segments, it should be possible to vary the relative impact of either amorphous or crystalline mechanisms, and in this way to tune the SMPU properties.

The amorphous SMPU mechanism, described here in terms of a confinement tube within which the hard segments can either move freely at high temperature or be fixated at a low temperature, is affected

also by the processing of the SMPU in addition to chemical composition. For example, when the polymer network is highly entangled, the characteristic relaxation time of chain segments within the tube is longer, resulting in higher recovery temperature or equivalently longer recovery time. When electrospinning is conducted at high strain-rate, chain entanglements are partially lost, as witnessed by the faster recovery time of the electrospun SMPU compared to the bulk SMPU.

4. Conclusions

A catalyst-free SMPU was synthesized based on PCL-TDI-EG components. Due to the amount of solvent during synthesis, the synthesized SMPU displayed semi-crystalline characteristics. However, due to the type of the diisocyanate and the short EG chain extender, we observed the phenomenon of time-dependent amorphous characteristics, in which a heat treatment removes the crystalline phase and the resulting amorphous phase is stable for prolonged time that is followed by recrystallization. The stable amorphous SMPU, prior to recrystallization, provides the ability to complete a full shape-memory cycle in the amorphous state, thus, enables to isolate the existence of SIC. DSC, DMA and XRD measurements validate the amorphous properties of the heat-treated SMPU, and a comparison to the as-synthesized semi crystalline SMPU was conducted.

We showed that SIC was absent during the shape memory cycle, and do not function as a shape fixity mechanism. However, bulk SMPU performs well, with shape fixity and shape recovery of 89% and 93%, respectively. It is therefore concluded that in this type of SMPU the governing mechanism is an amorphous mechanism, dominated by the disordered morphology of the molecular chains induced by the type of the hard segments (TDI-EG). We also showed that chemically equivalent but more ordered structures, such as electrospun SMPU fibers, display small strain-induced crystallization under the same memory cycle, which might drive the additional crystallization mechanism to affect the shape-memory properties. We propose that the amorphous and crystalline mechanisms can work in parallel, and their relative contribution depends on the synthesis and processing conditions.

Although our experiments were conducted on a single type of synthesized polyurethane, our suggestion that both the amorphous and crystalline mechanism are working in parallel should apply to a wide range of synthesized SMPUs. At one end of the amorphous-crystalline spectrum, the current study demonstrates with high certainty the existence of a purely amorphous shape memory mechanism. At the other end of the spectrum, highly crystalline SMPUs are described in the literature as solely governed by crystalline shape memory mechanism. However, it is likely that the amorphous mechanism in such crystallized SMPUs still contributes to the fixation and recovery, because all SMPUs share the same hard-soft molecular morphology. The relative contribution of each shape memory mechanism can be tuned by changing the chemical composition of the soft and hard segments. For example, replacing the TDI by MDI would likely increase the SMPU crystallinity and the mobility of the hard segments, resulting in a more predominant crystalline mechanism. On the other hand, adding side groups such as methyl or bulkier molecules would likely suppress crystallinity and enhance hard segments interlocking, promoting a more predominant amorphous mechanism. Such tuning, particularly the identification of the contribution of each mechanism for a variety of SMPUs, should be investigated by further research.

The electrospun SMPU fibers displayed superior recovery and fixity (~100% and 97% respectively). Combined with a simple synthesis process, this spinning method can be practically applied to industrial purposes. We also showed that electrospun SMPU displayed a minimal SIC (0.44%). Whether such small crystalline phase can impact the shape-memory function remains an open topic for future research. While both electrospun and bulk SMPU are chemically equivalent, the variety of controllable parameters in electrospinning processing can enlighten the morphological and topological effects over the shape memory

mechanisms.

Declaration of competing interest

The authors declare that they have no known competing financial interests or personal relationships that could have appeared to influence the work reported in this paper.

CRediT authorship contribution statement

A. Nissenbaum: Conceptualization, Investigation, Methodology, Visualization, Writing - original draft, Writing - review & editing. **I. Greenfeld:** Conceptualization, Writing - review & editing. **H.D. Wagner:** Supervision, Resources, Writing - review & editing.

Acknowledgments

The authors thank Dr. Galit Zilberman and Nir Galili for their generous assistance in the shape memory cycle and time-dependent XRD measurements. This research was made possible in part by the generosity of the Harold Perlman family. H.D.W. is the recipient of the Livio Norzi Professorial Chair.

Appendix A. Supplementary data

Supplementary data to this article can be found online at <https://doi.org/10.1016/j.polymer.2020.122226>.

References

- [1] F. Pilate, A. Toncheva, P. Dubois, J.-M. Raquez, Shape-memory polymers for multiple applications in the materials world, *Eur. Polym. J.* 80 (2016) 268–294.
- [2] C. Liu, H. Qin, P.T. Mather, Review of progress in shape-memory polymers, *J. Mater. Chem.* 17 (2007) 1543.
- [3] J.H. Suman Thakur, in: *Asp. Ofg Polyurethane*, 2017, pp. 53–71, <https://doi.org/10.5772/32009>.
- [4] M. Bothe, Shape memory and actuation behaviour of semicrystalline polymer networks. https://inis.iaea.org/collection/NCLCollectionStore/_Public/46/001/46001488.pdf, 2014.
- [5] I.S. Gunes, F. Cao, S.C. Jana, Evaluation of nanoparticulate fillers for development of shape memory polyurethane nanocomposites, *Polymer (Guildf)*. 49 (2008) 2223–2234.
- [6] A. Lendlein, S. Kelch, Shape-Memory Effect from permanent shape, *Angew. Chem.* 41 (2002) 2034–2057.
- [7] A. Larranaga, E. Lizundia, Strain-induced crystallization, *Cryst. Multiph. Polym. Syst.* (2018), <https://doi.org/10.1016/B978-0-12-809453-2.00015-3>.
- [8] Y. Nie, Z. Gu, Y. Wei, T. Hao, Z. Zhou, Features of strain-induced crystallization of natural rubber revealed by experiments and simulations, *Polym. J.* 49 (2017) 309–317.
- [9] Masatoshi Tosaka, Syozo Murakami, Sirilux Poompradub, S. Kohjiya, Y. Ikeda, Shigeyuki Toki, Igors Sics, B.S. Hsiao, Orientation and Crystallization of Natural Rubber Network as Revealed by WAXD Using Synchrotron Radiation, 2004, <https://doi.org/10.1021/MA0355608>.
- [10] Y. Zhu, J. Hu, K. Yeung, Effect of soft segment crystallization and hard segment physical crosslink on shape memory function in antibacterial segmented polyurethane ionomers, *Acta Biomater.* 5 (2009) 3346–3357.
- [11] E.A. Pieczyk, M. Maj, K. Kowalczyk-Gajewska, M. Staszczak, A. Grady, M. Majewski, M. Cristea, H. Tobushi, S. Hayashi, Thermomechanical properties of polyurethane shape memory polymer-experiment and modelling, *Smart Mater. Struct.* 24 (2015) 45043.
- [12] W. Yan, L. Fang, U. Noechel, K. Kratz, A. Lendlein, Influence of deformation temperature on structural variation and shape-memory effect of a thermoplastic semi-crystalline multiblock copolymer, *Express Polym. Lett.* 9 (2015) 624–635.
- [13] N. Lamba, *Polyurethanes in Biomedical Applications*, Routledge, New York, 1998, <https://doi.org/10.1201/9780203742785>.
- [14] B.S. Lee, B.C. Chun, Y.-C. Chung, K. Il Sul, J.W. Cho, Structure and thermomechanical properties of polyurethane block copolymers with shape memory effect, *Macromolecules* (2001), <https://doi.org/10.1021/ma001842l>.
- [15] K. Tharanikkarasu, G. Radhakrishnan, Tetraphenylethane iniferters: polyurethane-polystyrene multiblock copolymers through “living” radical polymerization, *J. Appl. Polym. Sci.* 66 (1997) 1551–1560.
- [16] Y. He, X. Zhang, X. Zhang, H. Huang, J. Chang, H. Chen, Structural investigations of toluene diisocyanate (TDI) and trimethylolpropane (TMP)-based polyurethane prepolymer, *J. Ind. Eng. Chem.* 18 (2012) 1620–1627.
- [17] M. Sumi, Y. Chokki, Y. Nakai, M. Nakabayashi, T. Kanzawa, Studies on the structure of polyurethane elastomers. I. NMR spectra of the model compounds and some linear polyurethanes, *Makromol. Chem.* 78 (1964) 146–156.

- [18] G. Tian, G. Zhu, T. Ren, Y. Liu, K. Wei, Y.X. Liu, The effects of PCL diol molecular weight on properties of shape memory poly(ϵ -caprolactone) networks, *J. Appl. Polym. Sci.* 136 (2019) 47055.
- [19] D.I. Bower, W.F. Maddams, *The Vibrational Spectroscopy of Polymers*, Cambridge University Press, 1989, <https://doi.org/10.1017/CBO9780511623189>.
- [20] F.C. Wang, M. Feve, T.M. Lam, J.-P. Pascault, FTIR analysis of hydrogen bonding in amorphous linear aromatic polyurethanes. II. Influence of styrene solvent, *J. Polym. Sci., Part B: Polym. Phys.* 32 (1994) 1315–1320.
- [21] H. Hao, J. Shao, Y. Deng, S. He, F. Luo, Y. Wu, J. Li, H. Tan, J. Li, Q. Fu, Synthesis and characterization of biodegradable lysine-based waterborne polyurethane for soft tissue engineering applications, *Biomater. Sci.* 4 (2016) 1682–1690.
- [22] V.V. Vasil'ev, O.G. Tarakanov, A.I. Dyemina, A.I. Shirobokova, Crystallization study of polyurethanes, *Polym. Sci.* 8 (1966) 1031–1038.
- [23] S.K. Pollack, D.Y. Shen, S.L. Hsu, Q. Wang, H.D. Stidham, Infrared and x-ray diffraction studies of a semirigid polyurethane, *Macromolecules* 22 (1989) 551–557.
- [24] P.J. Stenhouse, E.M. Valles, S.W. Kantor, W.J. Macknight, Thermal and rheological properties of a liquid-crystalline polyurethane, *Macromolecules* 22 (1989).
- [25] C. Hepburn, *Polyurethane Elastomers*, 1992.
- [26] B. Bogdanov, V. Toncheva, E. Schacht, L. Finelli, B. Sarti, M. Scandola, Physical properties of poly(ester-urethanes) prepared from different molar mass polycaprolactone-diols, *Polymer (Guildf)*. 40 (1999) 3171–3182.
- [27] P. Ping, W. Wang, X. Chen, X. Jing, The influence of hard-segments on two-phase structure and shape memory properties of PCL-based segmented polyurethanes, *J. Polym. Sci., Part B: Polym. Phys.* 45 (2007) 557–570.
- [28] A.V. Salvekar, Y. Zhou, W.M. Huang, Y.S. Wong, S.S. Venkatraman, Z. Shen, G. Zhu, H.P. Cui, Shape/temperature memory phenomena in un-crosslinked poly- ϵ -caprolactone (PCL), *Eur. Polym. J.* 72 (2015) 282–295.
- [29] J. Lal, J.E. Mark, American chemical society. Division of polymer chemistry. & American chemical society, Meeting (190th, in: Chicago, I. . *Advances in Elastomers and Rubber Elasticity*, Plenum Press, 1985, 1986, https://books.google.co.il/books?id=agr3BwAAQBAJ&dq=TDI+MDI+strain+induced+crystallization&hl=iw&source=gbs_navlinks_s.
- [30] M. Walczak, *Role Prop. Confin. Amorph. phase Polym.*, PhD thesis, 2012, <https://doi.org/10.1145/3300001.3300014>.
- [31] M. Sáenz-Pérez, E. Lizundia, J.M. Laza, J. García-Barrasa, J.L. Vilas, L.M. León, Methylene diphenyl diisocyanate (MDI) and toluene diisocyanate (TDI) based polyurethanes: thermal, shape-memory and mechanical behavior, *RSC Adv.* 6 (2016) 69094–69102.
- [32] Y. Ziming, H. Guanru, Y. Zhuohong, *Synthesis of Shape Memory Polyurethane Using Bulk Polymerization*, vol. 7493, 2017, pp. 1–6.
- [33] I. Greenfeld, X. Sui, H.D. Wagner, Stiffness, strength, and toughness of electrospun nanofibers: effect of flow-induced molecular orientation, *Macromolecules* 49 (2016) 6518–6530.
- [34] I. Greenfeld, E. Zussman, Polymer entanglement loss in extensional flow: evidence from electrospun short nanofibers, *J. Polym. Sci., Part B: Polym. Phys.* 51 (2013) 1377–1391.
- [35] F. Zhang, Z. Zhang, T. Zhou, Y. Liu, J. Leng, Shape memory polymer nanofibers and their composites: electrospinning, structure, performance, and applications, *Front. Mater.* 2 (2015) 62.
- [36] P.G. de Gennes, *Scaling Concepts in Polymer Physics*. Br. J. Psychiatry, vol. 112, Cornell University Press, 1979.
- [37] J. Blackwell, M.R. Nagarajan, T.B. Hoitink, Structure of polyurethane elastomers: effect of chain extender length on the structure of MDI/diol hard segments, *Polymer (Guildf)*. 23 (1982) 950–956.
- [38] K. Kojio, M. Furukawa, Y. Nonaka, S. Nakamura, Control of mechanical properties of thermoplastic polyurethane elastomers by restriction of crystallization of soft segment, *Materials (Basel)* 3 (2010) 5097–5110.